

NMR and Solvent Effect Study on the Active Site of Oxidized Azurin

K. Shahanipour¹, T. Nejad Satari², F. Mollaamin⁴ and M. Monajjemi^{3,*}

¹ Ph.D. student, Science and Research Branch, Islamic Azad University, Tehran, Iran

² Department of Biology, Science and Research Branch, Islamic Azad University, Tehran, Iran

³ Department of Chemistry, Science and Research Branch, Islamic Azad University, Tehran, Iran

⁴ Department of Chemistry, Qom Branch, Islamic Azad University, Qom, Iran

ABSTRACT

We have evaluated the NMR shielding tensors for active site of oxidized azurin. Azurin is classified to a type I copper protein with ET functionality. We have computed NMR shielding tensors at B3LYP and HF levels by using 6-31G basis set in the gas phase and in different solvents such as water, DMSO, Nitromethane, methanol, ethanol, acetone, dichloroethane. These solvents represent a wide range of solvent properties from the point of view of polarity as well as hydrogen bonding interactions. The NMR shielding tensors were calculated using the GIAO and CSGT methods. Our results reveal that NMR chemical shielding parameters are strongly affected by inducing different solvent media. Regarding to our plotted graphs of σ_{iso} , σ_{anis} , $\Delta\sigma$, η , δ versus ϵ , the largest σ_{iso} values obtained in ethanol and water for Cu atom whereas the smallest one belonged to DMSO. It is interesting to note that the opposite trend have been observed for asymmetry parameters (η).

Also, calculations at the HF in CSGT and GIAO methods have shown that molecular geometry and shielding properties are better than the other methods, B3LYP in GIAO and CSGT methods.

Keywords: Azurin; NMR parameters; Blue copper protein; Solvent effect

INTRODUCTION

The metalloproteins have attracted considerable interest among many researchers because of their various functionalities, such as electron transfer (ET), redox reaction, oxygen transportation, and activation. Blue copper protein is one of metalloproteins, which can be classified into three types on the basis of spectroscopic properties.

Type I copper protein has an absorption peak near 592-625 nm; type II copper protein has a similar peak to that of the general Cu(II) complex. Type III copper protein exhibits antiferromagnetism and has an absorption peak near 300 nm.

Azurin is classified to a type I copper protein with

ET functionality. The active site of azurin consists of one copper ion and five ligand residues: Gly 45, His46, Cys112, His117, and Met121. The copper ion is strongly coordinate-bonding to His46, Cys112, and His117, and bonds weakly to other residues [1].

The Cu site has a distorted trigonal geometry that is intermediate between that preferred by Cu(I) complexes (tetrahedral) and that preferred by Cu(II) complexes (tetragonal). Thus, the change in geometry with redox is limited, and the energy required for this structural rearrangement is small [2]. These observations

*Corresponding author: m_monajjemi@yahoo.com

led to the induced rack theory [3] and the entatic state theory[4], based on the hypotheses that the protein matrix forces the Cu(II) site into a catalytically poised geometry similar to the Cu(I) geometry. These theories, which trace the peculiar properties of the cupredoxins and their electron transfer capability back to the strained geometry of their active site, have been challenged recently[5,6], and the issue has been addressed through different theoretical methods.



Fig.1 Overview of the second structure of azurin. The active site consists of the copper ion and five ligand residues: Gly45, His46, Cys112, His117, and Met121[1].

Ryde et al.[5,6] performed quantum-mechanical(QM) optimization in vacuo of the geometry of the oxidized and reduced Cu sites, using the B3LYP hybrid density functional (DFT) method[6,7]. Surprisingly, the results of the calculations on the copper site were in clear contrast with the rack and entatic state hypotheses. The in vacuo optimized geometry of the isolated Cu(II) site was highly similar to the experimental geometry of the site in the protein structure. This suggested that the geometry of the Cu (II) site in cupredoxins is not strained by the protein matrix [8, 9].

Swart investigated the electronic structure of the active site of azurin by density functional

theory (DFT) and carried out MD simulation using the results.

Sugiyama et al.[1] have also carried out MD simulation of oxidized and reduced azurins and have analyzed their backbone dynamics. Nuclear magnetic resonance (NMR) spectroscopy is a valuable technique for obtaining chemical information. This is because the spectra are very sensitive to changes in the molecular structure. This name sensitivity makes NMR a difficult case for molecular modeling [10-12].

NMR spectroscopy is a powerful tool for study the structure dynamics and interaction of biological molecule such as protein and nucleic acids in solution [13-16].

As we know the effect of solvent molecules on proteins plays an important role in the chemical behavior of them and the effects span a considerable range and are governed primarily by solvent polarity. So in our current research, we have theoretically studied the effects of DMSO, nitromethane, methanol, ethanol, acetone, dichloroethane, water and gas phase on the chemical shielding parameters of ^{13}C , ^{15}N , ^{17}O , ^{64}Cu , ^{32}S nuclei involving in active site and its structural stability. The Gauge Including Atomic Orbitals (GIAO) and Continuous Set of Gauge Transformations (CSGT) approaches within the SCF-Hartree-Fock and B3LYP approximation have been used in order to investigate the influence different solvent media on the magnetic shielding tensors through Hartree-Fock and B3LYP approximation using 6-31G basis set. This basis set seems proper, because the CPU-consuming calculations using the HF method generally inhibit its application for NMR calculations of biological macromolecules with large basis sets.

COMPUTATIONAL DETAILS

In the present work, extensive quantum extensive quantum mechanical calculation of electronic structure of the active site of oxidized azurin (Fig.1) and solvent effects on ^{13}C , ^{15}N , ^{17}O , ^{64}Cu , ^{32}S -NMR parameters have been performed in different solvent media and in two available methods using GAUSSIAN 98 program.

We have studied the influence of DMSO, nitromethane, methanol, ethanol, acetone, dichloroethane, water and gas phase on

chemical shielding tensors. There are different methods of salvation. One family of models for systems in solution is referenced to as Self-Consistent Reaction Field (SCRF) method. The simplest SCRF model is the onsager reaction field model. For the simulation of a polar environment, this model was used as implemented in GAUSSIAN 98. In this model the solvent is consider as a uniform dielectric with a given dielectric constant.

At first, we have modeled the active site of azurin with chem. Office package and then optimized at the Hartree-Fock and B3LYP levels of theory with 6-31G basis set.

In view of the fact that the results of our earlier works [17-18] proved that addition of a greater number of polarization functions and extension of the basis set did not lead to a significant improvement of the results, the choice

of the middle basis set 6-31G was in our opinion justified.

After fully optimization of active site, we have calculated NMR parameters using the density functional B3LYP and HF method by Gauge Including Atomic Orbitals (GIAO) and Continuous Set of Gauge Transformations (CSGT) and have been reported in table 1(a,b,c). For more investigation of solvent effect, the graphs of obtained NMR parameters versus dielectric constant have been evaluated.

RESULTS AND DISCUSSION

In figs. 2-4, chemical shift anisotropy asymmetry (η), isotropy (σ iso), anisotropy (σ anisu), and $\Delta\sigma$ and chemical shift tensor (δ) are observed for ^{13}C , ^{15}N , ^{17}O , ^{64}Cu , ^{32}S nuclei in active site of oxidized azurin with respect to dielectric constants.

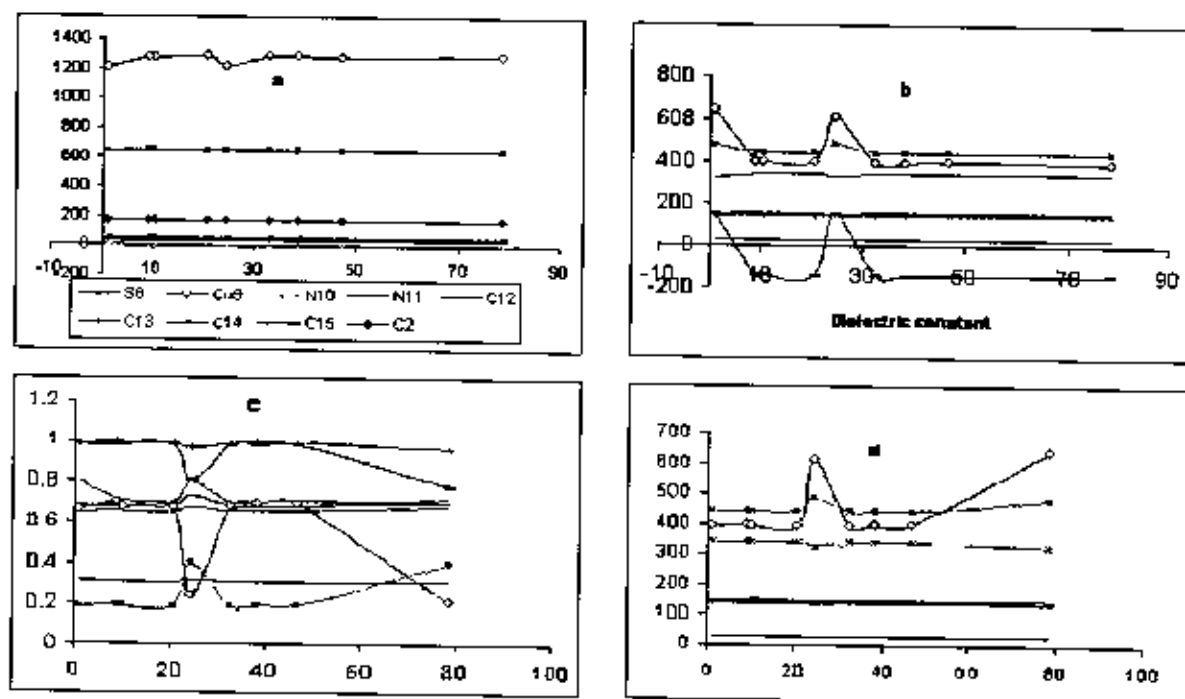


Fig. 2. The graphs of a) isotropic shielding values (σ iso), b) indirect shielding ($\Delta\sigma$), c) asymmetry parameters (η), d) anisotropic shielding value (σ anisu), of propane atoms of active site azurin in different solvent media at the level of HF/6-31G theory in CSGT method.

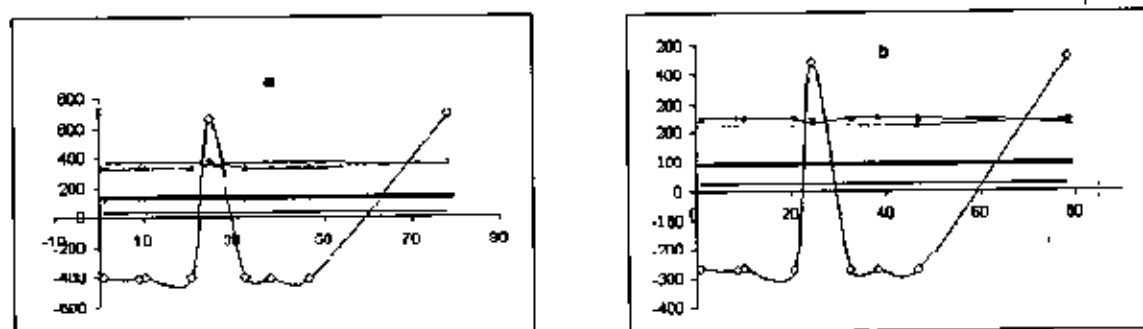


Fig. 3. The graphs of a) indirect shielding ($d\sigma$), b) chemical shift tensor δ_i , of propose atoms of active site azurin in different solvent media at the level of HF/6-31G theory in GIAO method

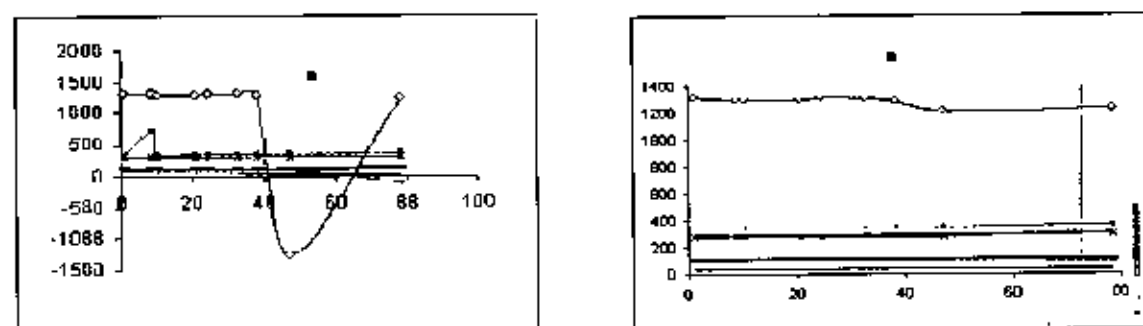


Fig. 4. The graphs of a) isotropic shielding values (σ_{iso}), b) chemical shift tensor δ_i , of propose atoms of active site azurin in different solvent media at the level of B3LYP/6-31G theory in CSGT method.

In the basis of the above diagrams, table 1(a,b,c) list values of the σ_{iso} , σ_{aniso} , $\Delta\sigma$, δ , η values for ^{13}C , ^{15}N , ^{17}O , ^{64}Cu , ^{32}S nuclei in different dielectric constants

As expected, the NMR shielding tensors of ^{13}C , ^{15}N , ^{17}O , ^{64}Cu , ^{32}S nuclei are drastically affected by what it is bonded to and the type of bond to its neighbor. Our obtained results yielded strong evidence that intermolecular effects such as electron transfer interactions play very important role in determining the ^{13}C , ^{15}N , ^{17}O , ^{64}Cu , ^{32}S -NMR chemical shielding tensors of active site of oxidized azurin and some systematic trends appeared from the analysis of the calculated values.

On the basis of both geometrical positions of ^{13}C , ^{15}N , ^{17}O , ^{64}Cu , ^{32}S existing in active site of oxidized azurin and computed results, for nuclei involved in electron transfer the obtained NMR parameters are not the same as those computed for other atoms.

For Cu_9 atom which behaves as electron donor, the σ_{iso} component showed the largest intermolecular effects and it shows positive shielding values, i.e, the electron transfer interaction produced a deshielding in this position.

Comparison of σ_{iso} , σ_{aniso} , $\Delta\sigma$ and δ values of Cu_9 atom with another shielding values in table 1 and also analysis of graphs of σ_{iso} , σ_{aniso} , $\Delta\sigma$ and δ 's versus dielectric constant exhibited in figs 2-4 revealed that, the largest values observed for ethanol and water, whereas the smallest belongs to DMSO. It is interesting to note that on the contrary, the opposite trend have been observed for asymmetry parameter (η). This logical behavior may be readily understood in accord with biological conceptions.

The metal ion in the electron-transfer copper proteins such as the type I copper proteins has been proposed to exist in an entatic state. These studies as well as earlier reports suggest that the metal-ligand interactions in the blue copper proteins indeed play an important role in imparting extra stability to the metal binding site of the protein[19].

Table 1. NMR parameters of C, N, O, Cu, S nuclei involving in active site azurin in different solvent media at the levels of RHF/6-31G and B3LYP/6-31G theory in GIAO and CSGT methods (a), (b), (c)

Solvent	Method	Atoms	GIAO					CSGT				
			σ_{iso}	σ_{anis}	$\Delta\sigma$	η	δ	σ_{iso}	σ_{anis}	$\Delta\sigma$	η	δ
78.39	HF B3LYP	C2	187.18 169.76	34.14 37.91	34.14 37.91	0.5276 0.5377	22.763 25.277	173.85 157.68	28.197 32.883	28.197 32.883	0.6812 0.627	18.748 21.869
		S6	740.4 566.54	332.09 344.81	332.09 344.81	0.3817 0.68	221.397 229.876	651.4 498.75	442.155 432.355	442.16 432.36	0.185 8.5289	294.77 288.237
		Cu9	1758.5 168.64	260.43 1312.34	-405.19 1312.34	0.285 0.9158	-270.13 874.895	1292.3 413.49	994.373 1151.17	394.38 -1058.5	0.666 0.694	262.915 -905.666
		N10	8.25 21.45	361.85 275.11	361.84 275.11	0.351 0.1024	241.229 183.305	14.294 11.892	332.85 256.303	332.85 256.3	0.29 0.1327	221.9 170.868
		N11	8.23 24.56	369.04 298.67	369.83 298.67	0.3577 8.184	246.022 199.112	13.62 11.968	341.554 275.877	341.55 275.88	0.3059 0.1984	227.702 183.918
		C12	55.32 47.46	146.41 122.03	146.41 122.03	0.6943 0.557	97.603 81.35	38.938 33.438	154.349 129.223	154.35 129.22	0.6529 0.472	102.899 86.149
		C13	62.89 65.7	127.57 90.95	127.56 90.95	8.9525 0.9493	85.043 60.635	34.052 39.791	140.947 103.257	140.95 -103.3	0.9967 0.9902	93.965 -68.865
		C14	61.83 59.19	138.47 189.55	138.47 109.55	0.7494 0.6586	92.315 73.035	35.035 43.766	146.58 119.154	148.58 119.15	0.7003 0.5946	99.054 79.436
		C15	62.68 58.01	128.79 182.07	129 182.07	0.9713 0.8136	85.86 68.047	34.131 33.508	141.648 111.963	-142.58 111.96	0.9864 0.8837	-95.055 74.642
		46.8	HF B3LYP	C2	187.23 169.85	34.17 37.81	34.17 37.81	0.5278 0.5315	22.778 25.207	173.85 157.75	28.222 32.721	28.224 32.721
S6	739.9 565.8			332.83 341.47	332.83 716.01	0.382 0.678	221.88 227.647	650.75 497.87	443.025 428.762	443.83 428.76	0.1899 0.5285	295.35 285.84
Cu9	1744.4 169.81			262.51 1288.84	-413.12 1298.84	0.27 0.925	-275.41 865.59	1282.9 -413.19	400.404 1139.48	400.4 -1351	0.6963 0.6868	266.936 -900.67
N18	8.59 21.75			361.62 276.03	361.62 276.03	0.3496 0.1022	241.079 184.019	-11.896 12.081	332.385 257.174	332.38 257.17	0.29 0.1275	221.59 171.45
N11	8.83 24.5			368.08 299.14	368.09 299.14	8.3539 0.1865	245.388 199.42	-13.03 14.864	340.546 275.946	340.55 275.95	0.3019 0.1991	227.03 183.963
C12	55.41 47.4			146.29 122.19	146.29 122.19	0.6991 0.556	97.527 81.46	39.024 33.386	154.166 129.318	154.17 129.32	8.658 0.47	102.778 86.212
C13	62.92 65.51			127.33 91.01	127.33 91.01	8.9548 8.9506	84.885 60.676	34.124 39.603	140.641 103.264	140.64 -103.41	0.9983 0.9972	93.761 -68.938
C14	62.05 58.24			138.21 188.48	138.21 109.48	0.7535 8.66	92.142 72.985	45.196 43.792	148.341 119.882	148.34 119.08	0.7044 0.5955	98.804 79.389
C15	62.73 58.02			128.77 102.18	128.77 102.18	0.9695 0.8124	85.848 68.118	34.203 33.51	141.523 111.959	-142.27 111.96	8.9895 0.8835	-94.846 74.639
38.215				C2	187.19 169.77	34.15 37.89	34.15 37.9	0.5277 0.5134	22.764 25.263	173.86 157.67	28.2 32.796	28.2 32.796
		S6	740.31 585.82	332.18 343.04	332.18 343.04	0.38188 0.677	221.451 228.695	651.3 498.12	442.237 438.164	442.24 430.16	0.186 0.528	294.825 286.776
		Cu9	1749.8 172.16	260.97 1294.77	-406.52 1294.77	0.2838 0.9235	-271.02 863.18	1291 -410.35	995.214 1137.09	395.22 -1346	0.672 0.689	263.476 -897.343
		N10	8.29	361.83	361.83	0.3509	241.22	-14.247	332.787	332.79	0.291	221.858

Table I. Continue.

(b)

			21.75	276.17	276.17	8.1025	184.115	12.05	257.34	257.34	0.126	171.56
	HF B3LYP	N11	8.35	368.88	368.88	0.3569	245.92	-13.509	341.39	341.39	0.3051	227.594
			24.24	298.99	298.99	0.1891	199.33	14.704	276.192	276.19	0.1998	184.129
		C12	55.34	146.39	146.39	0.695	97.592	38.952	154.319	154.32	0.653	102.879
			47.36	122.23	122.23	0.5566	81.487	33.341	129.357	129.36	0.4709	86.238
		C13	62.9	127.52	127.52	0.953	85.017	34.067	140.896	140.9	8.997	93.93
			65.44	91.03	91.03	0.9486	60.684	39.55	103.287	-183.35	0.9987	-68.902
		C14	61.87	138.43	138.43	0.7581	92.285	45.858	148.541	148.54	8.7009	99.027
			58.26	109.4	109.48	0.6611	72.987	43.822	119.077	119.08	0.5961	79.385
		C15	62.7	128.78	128.78	0.971	85.856	34.147	141.623	-142.53	0.9873	-95.818
			57.96	102.19	102.23	0.8125	68.128	33.457	112.054	112.05	0.8825	74.703
		C2	187.2	34.15	34.15	8.5279	22.765	173.86	28.201	28.281	8.6616	18.881
			169.74	37.9	37.9	0.5349	25.268	157.66	32.8	32.8	0.6251	21.867
		S6	740.29	332.25	332.25	0.381	221.5	651.28	442.317	442.32	0.186	294.878
			585.78	343.28	343.28	0.673	228.852	498.23	430.587	430.59	0.5249	287.058
		Cu9	1749.6	261.05	-406.89	0.283	-271.26	1290.6	395.729	395.73	8.672	263.819
			174.64	1294.14	1294.14	0.9193	862.76	-407.93	1139	-1341.8	8.697	-894.557
		N10	8.33	381.82	361.82	0.3507	241.215	-14.212	332.769	332.77	8.2913	221.846
			21.61	276.18	276.19	8.1827	184.13	12.112	257.297	257.3	0.1261	171.53
		N11	8.36	368.85	368.85	0.3568	245.902	-13.498	341.353	341.35	0.305	227.569
			24.33	299.58	299.58	0.1889	199.72	14.652	276.22	276.22	0.1982	184.147
		C12	55.35	148.36	146.38	0.6952	97.586	38.959	154.306	154.3	0.6539	102.87
			47.33	122.24	122.25	0.556	81.495	33.328	129.35	129.35	8.4702	86.233
		C13	62.9	127.51	127.51	0.953	85.009	34.069	140.881	140.88	0.9971	93.921
			65.42	81.1	81.1	0.947	60.736	39.546	103.339	103.34	0.9999	68.893
		C14	61.88	138.42	138.41	0.7503	92.28	45.064	148.534	148.53	0.7011	99.023
			59.24	189.43	109.43	0.6632	72.954	43.8	119.028	119.03	0.598	79.352
		C15	62.7	128.78	128.78	0.9711	85.856	34.154	141.616	-142.52	0.9873	-95.01
			57.95	102.32	182.32	0.807	68.211	33.421	112.071	112.07	0.8767	74.714
		C2	184.25	34.5	34.5	0.5652	22.998	171.17	28.435	28.434	0.7339	18.956
			169.7	87.98	37.99	0.539	25.323	157.61	32.865	32.865	0.6277	21.91
		S6	729.6	371.08	371.88	0.502	247.38	645.52	487.887	487.08	8.398	324.725
			566.11	344.66	344.66	6.68	229.77	498.61	431.968	431.97	8.5382	287.979
		Cu9	1857.8	655.76	655.76	0.7365	437.172	1220.8	612.212	612.21	0.2398	408.142
			178.81	1311.36	1311.36	0.918	874.239	-412.36	1151.19	-1358.5	0.6948	-905.634
		N10	21.85	347.64	347.64	0.279	231.76	-2.035	320.209	320.21	8.248	213.47
			21.69	276.86	276.06	0.1019	184.639	12.027	257.183	257.18	0.1274	171.455
		N11	17.25	358.88	358.88	0.353	233.923	-5.534	325.345	325.35	8.3094	216.897
			24.41	286.63	298.63	0.1864	199.838	14.881	275.98	275.98	8.1978	184.867
		C12	55.49	144.84	144.84	8.7209	96.561	38.859	153.236	153.23	0.6717	102.157
			47.4	122.14	122.14	0.5566	81.427	33.368	129.264	129.28	0.4712	86.189
		C13	61.87	125.85	125.85	0.9132	83.898	32.922	139.49	139.49	6.9732	92.943
			65.53	91.81	91.01	0.9495	60.671	39.648	103.259	-103.33	0.9987	-68.883
		C14	66.96	131.58	131.58	0.8608	87.718	49.221	143.128	143.13	0.8003	95.414
			59.29	109.51	109.51	0.6608	73.006	43.844	119.107	119.11	0.5959	79.405
		C15	55.34	138.75	138.75	0.7238	92.502	28.178	149.955	149.96	0.3082	99.97
			57.98	182.21	162.21	0.8117	68.141	33.473	112.076	112.08	6.8812	74.717
		C2	187.21	34.15	34.15	0.5279	22.768	173.87	28.206	28.206	0.6817	18.804
			169.78	37.91	37.91	0.538	25.275	157.68	32.809	32.809	0.6272	21.873
		S6	748.2	332.37	332.37	0.38169	221.583	651.16	442.472	442.47	0.1869	294.98
			567.34	345.75	345.76	0.677	230.5	499.53	413.166	433.17	0.527	289.777
		Cu9	1748.3	261.53	-408.53	0.2803	-272.36	1288.7	396.964	396.97	0.679	264.643
			170.32	1386.63	1306.83	0.92	871.22	-412.51	1145.55	-1355.8	8.689	-903.88

Table I. Continuc..

(c)

	HF B3LYP	N10	8.39 21.48	361.79 274.81	361.79 274.91	0.3504 0.102	241.195 183.273	-14.129 11.912	332.686 256.083	332.68 256.08	0.291 0.1326	221.791 170.722
		N11	8.48 24.49	368.68 298.75	368.67 298.75	0.356 0.1855	245.784 199.165	-13.38 14.957	341.163 276.058	341.16 276.06	0.3041 0.1994	227.442 184.039
		C12	55.38 47.44	146.36 121.97	146.36 121.97	0.6961 0.558	97.57 81.312	38.975 33.422	154.27 129.182	154.27 120.18	0.6549 0.473	102.847 86.121
		C13	62.91 65.78	127.47 90.98	127.47 90.98	0.9535 0.9482	84.977 60.657	34.084 30.836	140.819 103.276	140.82 103.28	0.9974 0.9999	93.88 68.851
		C14	61.92 59.25	138.37 109.58	138.37 109.58	0.7511 0.6582	92.244 73.057	45.095 43.818	148.485 119.172	148.49 119.17	8.7819 0.594	98.99 79.448
		C15	62.71 57.88	128.78 182.1	128.78 102.08	0.9708 0.8132	85.851 68.066	34.17 33.493	141.588 112.003	-142.45 112	0.9878 0.8829	-94.967 74.669
10.36	HF B3LYP	C2	187.22 168.73	34.18 37.95	34.16 37.95	0.5279 0.5436	22.776 25.3	173.81 157.63	28.218 32.83	28.218 32.83	0.6815 0.6326	18.812 21.887
		S6	738.94 568.08	332.74 350.16	332.73 358.16	0.3819 0.675	221.82 233.44	650.81 500.12	442.928 436.46	442.93 436.46	0.189 0.528	295.285 290.97
		Cu9	1745.2 166.86	262.11 1285.58	-412.26 1285.57	0.2715 -0.9658	-274.84 857.85	1284.2 -417.61	399.489 1123.84	399.49 -1362.1	0.6933 8.65	266.326 -908.081
		N10	8.57 21.67	361.65 275.69	361.65 275.69	0.3496 8.1013	241.1 183.796	-13.923 11.973	332.448 256.915	332.45 256.91	0.2902 0.1277	221.632 171.277
		N11	8.75 24.54	368.22 298.83	368.22 208.83	0.3543 8.1818	245.479 199.219	-13.114 14.973	340.681 275.93	340.68 275.93	0.3023 0.1969	227.12 183.953
		C12	55.4 47.39	146.31 122.15	146.31 122.15	0.6984 0.556	97.538 81.433	39.011 33.372	154.191 129.31	154.19 129.31	8.6573 0.4703	102.794 86.207
		C13	62.92 65.48	127.35 91.09	127.35 91.09	0.9546 0.9476	84.901 60.73	34.115 30.587	140.677 103.343	140.68 -103.38	0.9981 0.9993	93.785 -68.917
		C14	62.81 59.15	138.25 109.37	138.25 109.37	0.7529 0.659	92.166 72.91	45.17 43.75	148.375 118.987	148.38 118.99	0.7038 0.5943	98.917 79.321
		C15	62.74 58.21	128.77 101.75	128.77 101.71	0.9699 8.8177	85.843 67.832	34.201 33.694	141.529 111.646	-142.31 111.65	8.989 0.8867	-94.871 74.431
		-	HF B3LYP	C2	184.26 178.64	34.18 38.12	34.18 38.12	0.57 0.599	22.785 25.413	171.18 158.12	28.335 33.3	28.339 33.3
S6	728.54 885.61			364.7 385.21	364.7 365.21	0.4999 8.473	243.136 243.471	644.67 540.91	480.694 456.891	480.69 456.89	0.3965 0.38	328.462 304.594
Cu8	1649.7 485.5			878.57 1231.35	678.57 1231.35	0.70187 0.287	452.38 820.9	1214.1 -87.266	644.831 1152.54	644.85 1152.5	0.2139 0.62	429.887 768.356
N18	20.94 31.67			348.04 293.44	348.04 293.44	0.2799 0.179	232.03 195.629	-2.06 16.801	320.544 270.447	320.54 270.44	0.248 8.0537	213.696 180.298
N11	18.33 25.25			349.48 305.08	349.4 305.09	8.3499 0.262	232.936 203.393	-4.61 11.499	323.97 281.465	323.97 281.47	8.3114 0.194	215.98 187.644
C12	55.25 58.82			144.9 123.87	144.9 123.87	0.7266 0.544	96.599 82.578	38.656 35.509	153.34 130.295	153.34 130.29	0.6756 0.467	102.226 86.863
C13	61.87 69.13			126.17 87.58	126.17 -90.24	0.9072 0.941	84.111 -60.159	32.976 41.887	139.737 98.925	139.74 -105.14	0.9653 0.8817	93.158 -70.095
C14	67.21 63.99			131.65 110.19	131.65 110.19	0.8505 0.687	87.765 73.458	49.464 47.499	143.161 119.074	143.16 119.07	0.8009 0.6224	95.441 79.383
C15	54.25 60.68			148.15 186.38	140.15 108.38	0.6902 0.6803	93.433 72.254	27.209 34.516	151.195 117.446	151.2 117.45	0.7794 8.784	100.797 78.298

The metal ion in the electron-transfer copper proteins such as the type I copper proteins has been proposed to exist in an entatic state. These studies as well as earlier reports suggest that the metal-ligand interactions in the blue copper proteins indeed play an important role in imparting extra stability to the metal binding site of the protein[19].

As expected, after Cu_0 , S_6 shows positive shielding values. Cys 112 is among the ligand residues the one that more strongly hybridizes with the Cu orbitals. The covalency of the copper-ligand bonds is very anisotropic and it was suggested that this should favor hole super exchange pathways that couple to the Cu through the Cys112 ligand[20]. The cysteine ligand decreases the reorganization energy. This decrease is caused by the transfer of charge from the negative charged thiolate group to CuII, which makes the oxidized and reduced structures quite similar[21].

For both N_{10} and N_{11} atoms which are fused in imidazole ring, shielding tensors are close to each other but according to our obtained results of fig. 2, as the dielectric constant in passing from the nitromethane to water, the σ_{aniso} and $\Delta\sigma$ of N_{11} and N_{10} increase and the η decrease in the ethanol which is expected to result in a significant shielding of this nitrogen nuclei at the Hartree-Fock level of theory with CSGT method.

Nitrogen ligands give up an appreciably lower reorganization energy than water, owing to the lower Cu-N force constant[21].

Figure 4 shows that, as the dielectric constant of the solvent increases, the $\Delta\sigma$ and σ_{aniso} of C_{15} and C_{13} increase and the η of C_{15} and C_{13} decreased in the ethanol at the Hartree-Fock level of theory with GIAO method.

Also, calculations at the HF in CSGT method (Fig. 2) and the HF in GIAO method (Fig. 3) have shown that molecular geometry and shielding properties are better than the other methods, B3LYP in GIAO and CSGT methods(fig. 4).

CONCLUSION

The results reported in this paper indicates that it is possible to measure NMR tensors of various nuclei involving in biological compounds either in

gas phase or in the presence of different solvent molecules theoretically. Several conclusions can be made on the basis of the observed results of the present study. Such amount of theoretical data can provide us important insights into the nature of molecular structures in biological systems.

Our main findings from the point of view of solvent effects can be summarized as follows:

optimization at the HF level of theory provides a suitable computational model in terms of calculated NMR parameters and relative energies.

NMR parameters are very sensitive to small changes in molecular geometry and chemical environment exhibited significant sensitivity to the intramolecular interactions. So, our obtained theoretical results emphasized on the influence of the environment factors

The largest σ_{iso} value of mentioned nuclei at active site azurin observed for ethanol and water, whereas the smallest one belongs to DMSO. It is interesting to note that the opposite trend have been observed for asymmetry parameters(η). This usual behavior may be readily understood in accord with biotechnological conceptions.

The calculation of nuclear magnetic resonance (NMR) parameters using ab initio techniques seems to be a major and a remarkable tool for investigation of how variations of biological systems and provides information on the local environment of selected species and their next nearest neighbors. However, combination of NMR study embedded in solvent medium reveals a logical interpretation of the observed results.

In conclusion, we have shown that theoretical calculations can be used to successfully solve biochemical problems. In similarly with experimental methods, they involve assumptions and interpretation, and they have their limitations, but there are many problems that are best studied by theory. Thus, theoretical methods have become a competitive alternative to experiments for biochemical investigations.

REFERENCES

- [1] A. Sugiyama, K. Sugimori, T. Shuku, T. Nakamura, H. Saito, H. Nagao, H. Kawabe, K. Nishikawa. *Int J Quantum Chem.* 105, 2005, 588-595.
- [2] F. Rienzo, R. Gabdouliline, R. Wade, M. Sola, M. Menziani. *CMLS.* 61. 2004. 1123-1142.
- [3] B.G. Malmstrom. *Eur J Biochemistry* 223. 1994. 711-718.
- [4] R. J. P. Williams. *Eur J Biochem.* 234. 1995. 363-381.
- [5] U Ryde, M H Olsson, K Pierloot. *Theoretical and Computational Chem.* 9. 2001. 1-55.
- [6] U Ryde, M H Olsson, B O Roos, A C Borin. *Theor Chem Acc.* 105. 2001. 452-462.
- [7] M J Frisch, G W Trucks, A B Schlegel, P M Grill, B G Johnson, M A Robb. *GAUSSIAN 94, Gaussian 1994*, Pittsburgh, PA.
- [8] M. H. M. Olsson, *Theoretical studies of blue copper proteins*. Ph.D thesis, 2000.
- [9] U Ryde, M H Olsson, B O Roos, O A Kerpel, K Pierloot. *J Biol Inorg Chem.* 5. 2000. 565-574.
- [10] M Muhl. *Encycl Comput Chem.* 3. 1998. 1835.
- [11] C J Jameson, H J Osten. *Annual Reports on NMR spectroscopy.* 17. 1986. 1.
- [12] C J Jameson. *Annual Reports on NMR spectroscopy.* 21. 1989. 51.
- [13] B Furtin, C Richter, J H Schwalbe. *Chem Biochem.* 2003. 10-36.
- [14] S E Bucher, J M Burke. *Biochemistry.* 33. 1994. 992-999.
- [15] T J Warren, P B Moore. *J Biomol NMR.* 20. 2001. 311-323.
- [16] T J Warren, P B Moore. *J Biomol NMR.* 20. 2001. 311-323.
- [17] S A Mc Callum, A J Pardi, *J Mol Biol.* 325. 2003. 843-856.
- [18] M Monajjemi, S Ketabi, A Amiri. *Russ J Phys Chem.* 80. 2006. 55-62.
- [19] M. Monajjemi, A. Hadadi, B. Honarparvar, S. Irani, F. Mollaamin, A. Tahan. *The Egyptian J. of Biochemistry & Molecular Biology.* 26. 2008. 83-100.
- [20] A. Sujak, N. J. M. Sanghamitra, O. Maneg, B. Ludwig, S. Mazumdar. *Biophys. J.* 93. 2007. 2845-2851.
- [21] P. V. R. Schleyer, *Encyclopedia of Computational Chemistry* (Wiley, Chichester, 1998), Vol. 4. pp. 2547-2574.
- [22] U. Ryde, M. Olsson, K. Pierloot, Eriksson L. A, editor, Elsevier, Amsterdam. *Theoretical and Computational Chemistry.* 9. 2001. 1-5.

